JOURNAL OF GUIDANCE, CONTROL, AND DYNAMICS
Vol. 16, No. 3, May-June 1993

Optimal Open Multistep Discretization Formulas for Real-Time Simulation

Daniel D. Moerder*
NASA Langley Research Center, Hampton, Virginia 23665
and
Anthony J. Calise† and Paul Clemmons‡
Georgia Institute of Technology, Atlanta, Georgia 30332

The performance of digital real-time simulations is considered. A figure of merit is derived that quantifies a simulation's fidelity in terms of the time-domain discrepancy between its output and that of the plant it simulates, assuming that the plant is linearizable and asymptotically stable. This performance index is then used in deriving an easily automated procedure for calculating optimal values for free parameters in plant discretizations based on a generalized form of open linear multistep integration formulas. The theory is demonstrated in simulating the rigid-body dynamics of a fully articulated helicopter rotor blade system.

I. Introduction

REAL-TIME simulations are characterized by two important properties. First, the passage of time in the simulation takes place at the same rate as in the environment in which the simulation operates. Second, the simulation is required to accept inputs from and release outputs to analog processes, such as human operators.

Because of the first consideration, numerical techniques developed for the general problem of propagating systems of ordinary differential equations are not necessarily suitable for use in real-time simulations in which the plant state is propagated using a digital computer. First, their numerical integration algorithms must be causal; that is, when propagating the plant state from time t to $t+\Delta t$, the value of the state at $t+\Delta t$ must be available to the environment at that time. This tends to preclude using iterative schemes, such as predict/correct algorithms. Second, particularly as the complexity of the simulation grows, the computational overhead associated with calculating the plant state derivative dominates that associated with the integration procedure. This makes integration algorithms which use more than one derivative evaluation per time step, such as Runge-Kutta schemes, unattractive. On the other hand, open linear multistep integration algorithms such as the Adams-Bashforth formulas are structurally very well suited for simulator use, being causal and requiring only one state derivative calculation per time step. Unfortunately, their poor accuracy and stability properties are notorious.

The second consideration leads to complications because the plant discretization in a real-time simulation is a sampled data system. An input signal entering the discretized plant dynamics is subjected to, at least, a data hold. If the signal contains significant frequency content outside the Nyquist frequency associated with the integration stepsize, it is also necessary to prefilter it. An additional digital/analog reconstruction hold is required at the interface between the output of the discretized plant dynamics and the environment. All of this introduces phase and magnitude distortion effects which cannot be accommodated by any plant discretization scheme that merely seeks to propagate the plant dynamics accurately in discrete time.

These difficulties have been recognized for some time. The past 25 years have produced a number of studies[1-8] aimed at developing improved procedures for deriving discrete models for simulation of analog plants. In the largest single category of these,[1-3] the aim is to control the frequency response of the plant discretization. Reference 1 derives a procedure for synthesizing a discretization which minimizes a quadratic measure of disparity between the poles of the discretization and those of the z transform of the plant transfer function. In Ref. 2 an adaptation of root locus techniques from classical control theory is applied to the design of simulations consisting of a plant discretization with an output reconstruction hold. Reference 3 describes a class of tunable discrete integration formulas in which phase and gain characteristics of the discretization can be empirically adjusted to achieve desired frequency response. This procedure also considers output reconstruction in the design process.

The discretization design problem has also been examined from other points of view. A procedure is derived in Ref. 4 for optimizing the stability region, or maximum time step for which numerical stability is retained, in linear multistep integration formulas. References 3 and 5 develop an algorithm for discretizing highly nonlinear plants with multistep algorithms using transition matrix-like expressions based on local plant linearizations. Reference 7 describes an approach to deriving linear multistep integration algorithms in which the state derivative time history is assumed to be sinusoidal, rather than polynomial, as in the case of classical integration formulas. These integration formulas are intended for simulating systems whose response is dominated by oscillatory dynamics.

This paper provides three results. An analytical figure of merit is derived which characterizes the fidelity of a digital real-time simulation of a linearizable, time invariant, asymptotically stable plant with probabilistically distributed input signals and initial conditions. This "fidelity measure" is then used as a cost function to derive optimal parameter values in a generalized form of open one- and two-step linear multistep numerical integration formulas which would be used to propagate the plant state in the simulation. Finally, as an example, the theory is exercised in calculating optimized plant discretizations for simulating the rigid-body dynamics of a helicopter rotor blade.

It should be noted that the restriction of this theory to asymptotically stable plants is not as confining as it might first sound. Marginally stable dynamics, for design purposes, may

Presented at the AIAA Flight Simulation Technology Conference, Monterey, CA, Aug. 17-19, 1987; received Dec. 10, 1987; revision received May 5, 1992; accepted for publication Aug. 7, 1992.

*Senior Research Engineer, Spacecraft Control Branch.
†Professor, School of Aerospace Engineering.
‡Graduate Student, School of Aerospace Engineering.

be approximated as having very slight asymptotic stability. This is done in this paper's example. Unstable systems, if they are to be simulated in real time, are usually stabilized by an agency in the environment, such as a human operator. The simulation model can be made stable by representing that agency as part of the model.

II. Real-Time Simulation Performance

This section formulates a simulation fidelity performance criterion which is used as the cost function for optimal simulation design. The criterion is applicable in cases for which the plant and simulation dynamics are asymptotically stable and time invariant and where the input signal and environmental effects can be modeled as bounded stationary stochastic processes. Under these assumptions, it is meaningful to define the average mean-squared simulator error

$$e_{ss}^2 = \lim_{t\to\infty} \frac{1}{t} \int_0^t E\{e^T(s)e(s)\}\, ds \tag{1}$$

as a measure of steady-state simulation performance, where $e(t)$ is the simulator error, given by

$$e(t) = y(t) - \hat{y}(t) \tag{2}$$

In Eq. (2), $y(t)$ is the plant output and $\hat{y}(t)$ is the output of the simulator. The quantity e_{ss}^2 is a natural and intuitively appealing measure for comparing the steady-state frequency response of the simulation to that of the physical plant. It does not, however, directly reflect the quality of the transient response. Fidelity in transients can be considered using the homogeneous trajectory of $e(t)$ from a probabilistically distributed initial condition on the plant and simulation dynamics. In this case, an appropriate measure is the integral mean-squared transient error

$$e_t^2 = \lim_{t\to\infty} \int_0^t E\{e^T(s)e(s)\}\, ds \tag{3}$$

Since, in simulation design, both transient and steady-state response is of interest, we define our performance criterion as

$$J = (1-\alpha)e_{ss}^2 + \alpha e_t^2 \qquad \alpha \in [0, 1] \tag{4}$$

Fidelity measures similar to e_{ss}^2 and e_t^2 were examined in Ref. 8. In that study, however, the measures were based on the behavior of the simulator error at the sampling instants only, rather than across the sampling interval, so that the measures were not properly sensitive to continuous-time reconstruction effects.

To obtain a tractable expression for J, it will be assumed in the sequel that the plant to be simulated can be linearized, with perturbation dynamics

$$\dot{x} = Ax + Bu \qquad x \in \mathcal{R}^n \qquad u \in \mathcal{R}^m \tag{5}$$

$$y = Cx \qquad y \in \mathcal{R}^p \tag{6}$$

The system is further assumed to be driven by a stationary zero-mean Gaussian process described by

$$u = C_u x_u \tag{7}$$

$$dx_u = A_u x_u\, dt + B_u\, dw \qquad x_u \in \mathcal{R}^{n_u} \tag{8}$$

where dw is a Wiener process with

$$E[w(t)w^T(s)] = W\delta(t-s) \tag{9}$$

The transfer function of the prefilter on the simulation's input signal has the realization

$$u_f = C_f x_f \qquad u_f \in \mathcal{R}^m \tag{10}$$

$$dx_f = [A_f x_f + B_f u]\, dt + d\pi \tag{11}$$

for $x_f \in \mathcal{R}^{n_f}$, where A_f is asymptotically stable and π is measurement noise, assumed white, with covariance

$$E[\pi(t)\pi^T(s)] = \Pi\delta(t-s) \tag{12}$$

The dynamics of the discretized representation of the plant are given by

$$z_{k+1} = \Phi_I z_k + \Gamma_I \bar{u}_{f,k} + w_{I,k} \tag{13}$$

where $z \in \mathcal{R}^{n_z}$, the k subscript denotes the kth time step, and the term $\bar{u}_{f,k}$ generally takes the form

$$\bar{u}_{f,k}^T = [u_{f,k}^T : u_{f,k-1}^T : \cdots] \tag{14}$$

The disturbance term $w_{I,k}$ consists of aliasing and quantization error effects, which are modeled as white noise, with covariance

$$E\{w_{I,k}w_{I,j}^T\} = W_I\delta_{kj} \tag{15}$$

in the sequel. A discussion of the validity of this assumption is given in Ref. 8. The output of the simulation is expressed as

$$\hat{y}_k(\tau) = \hat{C}(\tau)z_k \qquad \tau \in [0, \Delta t) \tag{16}$$

where $\hat{y} \in \mathcal{R}^p$ and $\hat{C}(\tau)$ is some integrable function. Finally, for convenience, we assume that π, w, and w_I are mutually uncorrelated.

Using Eqs. (5–12), adjoin the plant, prefilter, and input signal dynamics to form

$$d\eta\, \bar{A}\eta\, dt + \bar{B}\, d\nu \tag{17}$$

where

$$\eta^T = [x_f^T : x^T : x_u^T], \qquad \nu^T = [\pi^T : w^T] \tag{18}$$

The plant output across the kth sampling interval is given by

$$y_k(\tau) = C_c\Phi_c(\tau)\eta_k + C_c w_{c,k}(\tau) \tag{19}$$

where

$$C_c = [0_{p\times n_f} : C : 0_{p\times n_u}] \tag{20}$$

$$\Phi_c(\tau) = \exp\{\bar{A}\tau\} \tag{21}$$

and $w_{c,k}(\tau)$ has covariance $W(\tau)$, given by

$$W_c(\tau) = E\{w_{c,k}(\tau)w_{c,k}^T(\tau)\} = \int_0^\tau \exp\{\bar{A}s\}\bar{B}K\bar{B}^T \exp\{\bar{A}s\}\, ds \tag{22}$$

$$K = \text{block diag}\{\Pi, W\} \tag{23}$$

Similarly, the discrete-time transition expression for η_k is

$$\eta_{k+1} = \Phi_c(\Delta t)\eta_k + w_{c,k}(\Delta t) \tag{24}$$

Next, adjoin the plant discretization dynamics to those of the plant itself to form

$$\bar{x}_k^T = [z_k^T : \eta_k^T] \tag{25}$$

Using Eqs. (13), (16), (19), (21), and (24), the error at the sampling instants propagates according to

$$e_k(0) = \bar{C}(0)\bar{x}_k \tag{26}$$

$$\bar{x}_{k+1} = \bar{\Phi}\bar{x}_k + \theta_k \tag{27}$$

where

$$\bar{C}(\tau) = \left[-\hat{C}(\tau) : C_c\Phi_c(\tau) \right] \tag{28}$$

In Eq. (27), $\bar{\Phi}$ has the structure

$$\bar{\Phi} = \begin{bmatrix} \Phi_I & \Phi_{I,\eta} \\ 0 & \Phi_c(\Delta t) \end{bmatrix} \tag{29}$$

where $\Gamma_{I,\eta}$ represents the influence of the prefiltered input signal in the discretization dynamics. The noise term θ_k is

$$\theta^T = \left[w_{I,k}^T : w_{c,k}^T \right] \tag{30}$$

with covariance

$$\Theta = E\{\theta_k\theta_k^T\} = \text{block diag}\{W_I, W_c\} \tag{31}$$

Note that, in cases where $\bar{u}_{f,k}$, from Eq. (14), contains components from the previous time step or earlier, the structure of η_k and $w_{c,k}$ must be modified slightly to accommodate the historical values of x_f. An example of this for two-step discretization (employing $\bar{u}_{f,k-1}$) is given in the next section.

Across the kth sampling interval, $e_k(\tau)$ is given by

$$e_k(\tau) = \bar{C}(\tau)\bar{x}_k + C_c w_{c,k}(\tau) \tag{32}$$

The simulation error is zero mean, with covariance

$$E\left\{e_k(\tau)e_k^T(\tau)\right\} = \bar{C}(\tau)P_k\bar{C}^T(\tau) + C_c W_c(\tau)C_c^T \tag{33}$$

where

$$P_{k+1} = \bar{\Phi}P_k\bar{\Phi}^T + \Theta \tag{34}$$

Given that $\bar{\Phi}$ is asymptotically stable, the steady-state solution of Eq. (34) is P_{ss}, where

$$\bar{\Phi}P_{ss}\bar{\Phi}^T - P_{ss} + \Theta = 0 \tag{35}$$

We next rewrite Eq. (1) as

$$e_{ss}^2 = \lim_{t\to\infty} \frac{1}{(N+1)\Delta t} \sum_{k=0}^{N} \int_0^{\Delta t} E\left\{e_k^T(s)e_k(s)\right\} ds \tag{36}$$

Using Eqs. (33–35), then,

$$e_{ss}^2 = \frac{1}{\Delta t}\left[\text{tr}\{P_{ss}M\} + \text{tr}\{M'\}\right] \tag{37}$$

$$M = \int_0^{\Delta t} \bar{C}^T(s)\bar{C}(s)\, ds \tag{38}$$

$$M' = C_c \int_0^{\Delta t} W_c(s)\, ds C_c^T \tag{39}$$

Note that only the first term in e_{ss}^2 is affected by the plant discretization. The second term describes the propagation of noise through the physical plant over the interval between the sampling instants.

In the transient case, $w_{c,k}(\tau) = 0$, and from Eq. (3),

$$e_t^2 = \lim_{N\to\infty} \sum_{k=0}^{N} \int_0^{\Delta t} E\left\{e_k^T(s)e_k(s)\right\} ds \tag{40}$$

Again, given that $\bar{\Phi}$ is asymptotically stable,

$$\lim_{N\to\infty} \sum_{k=0}^{N} E\left\{e_k(0)e_k^T(0)\right\} = \bar{C}(0)P_t\bar{C}^T(0) \tag{41}$$

where

$$\bar{\Phi}P_t\bar{\Phi}^T - P_t + X_0 = 0 \tag{42}$$

$$X_0 = E(x_0x_0^T) \tag{43}$$

From Eqs. (33), (38), (40), and (41), we have

$$e_t^2 = \text{tr}\{P_tM\} \tag{44}$$

so that the total performance J, from Eq. (4), is given by

$$J = \text{tr}\{PM\} + \frac{\alpha}{\Delta t}\text{tr}\{M'\} \tag{45}$$

where P is defined by $\varphi(P)$, given by

$$\varphi(P) = \bar{\Phi}P\bar{\Phi}^T - P + \left[\frac{1-\alpha}{\Delta t}\Theta + \alpha X_0\right] = 0 \tag{46}$$

III. Optimal Discretization Formulas

In this section, the fidelity criterion J from Eq. (45) is exploited as a cost function in optimally designing one- and two-step discretization with structures

$$\hat{x}_{k+1} = \hat{x}_k + \Delta t\, \mathfrak{B}_0\hat{x}_k' \tag{47}$$

and

$$\hat{x}_{k+1} = \hat{x}_k + \Delta t\left[\mathfrak{B}_0\hat{x}_k' + \mathfrak{B}_1\hat{x}_{k-1}'\right] \tag{48}$$

respectively, where

$$\mathfrak{B}_j = \text{diag}\{\beta_{j1}, \ldots, \beta_{jn}\} \qquad j = 0, 1 \tag{49}$$

and $\hat{x}_k'$ is the plant state derivative, calculated for $\hat{x}_k$ and u_k. The diagonal structure of the $\mathfrak{B}_j$ in Eqs. (47) and (48) permits selection of the β in Eq. (49) to tune the performance of the discretization for each element of the state vector individually. The preceding formulas are special cases of generalized open linear multistep integration formulas treated in Ref. 8, which examined their optimal design for a fidelity criterion based on the simulator output error at the sample instants rather than in continuous time, across the sampling interval.

Both of the formulas are consistent to zeroth order (see Ref. 9, pp. 169–187); that is, both will track a nonzero setpoint exactly. This is important because although the design theory is developed for linearizations of nonlinear systems, the discretizations are to be implemented using the nonlinear dynamics directly. We additionally require that the formula (48) be consistent to first order, so that it will exactly track a ramp. This requirement, expressed by the constraint

$$\mathfrak{B}_1 = I - \mathfrak{B}_0 \tag{50}$$

eliminates n degrees of freedom from Eq. (48) and was motivated by numerical difficulties experienced in Ref. 8, when Eq. (50) was not enforced. Because we will only be working with one $\mathfrak{B}$ matrix of free parameters in this analysis, the j notation, as defined in Eq. (49), will be suppressed in the sequel.

The free parameters in Eqs. (47) and (48) are isolated by rewriting $\bar{\Phi}$ from Eq. (29) as

$$\bar{\Phi} = \Phi + \Pi\mathfrak{B}N \tag{51}$$

where, for Eq. (47),

$$\Phi = \text{block diag}\{I_n, \Phi_c\} \tag{52}$$

$$\Pi^T = [I_n : 0] \tag{53}$$

$$N = [\Delta tA : \Delta tBC_f : 0] \tag{54}$$

and for Eq. (48),

$$\Phi = \left[\begin{array}{cc|cc|c|c} I_n & \Delta tA & 0 & \Delta tBC_f & & 0 \\ I_n & 0 & 0 & 0 & & \\ \hline & & \phi_f & 0 & 0 & \Gamma_{u,f} \\ & & I_{n_f} & 0 & & 0 \\ \hline & 0 & & & \phi_p & \Gamma_{u,p} \\ & & & & & \phi_u \end{array}\right] \tag{55}$$

$$\Pi^T = [I_n : 0] \tag{56}$$

$$N = [\Delta tA : -\Delta tA : \Delta tBC_f : -\Delta tBC_f : 0] \tag{57}$$

where I_q denotes the qth-order identity matrix. The ϕ matrices in Eq. (55) are obtained by partitioning Φ_c to correspond to the partitions of $\bar{A}$ in Eq. (17)

$$\Phi_c = \left[\begin{array}{c|c|c} \phi_f & 0 & \Gamma_{u,f} \\ \hline & \phi_p & \Gamma_{u,p} \\ \hline 0 & & \phi_u \end{array}\right] \tag{58}$$

The problem of choosing $\mathfrak{B}$ to minimize J subject to the constraint $\varphi(P)$ is posed by adjoining $\varphi(p)$ to the first term in Eq. (45) to form the Lagrangian

$$\mathfrak{L} = \mathrm{tr}\{PM\} + \mathrm{tr}\{\varphi(P)L^T\} \tag{59}$$

For convenience, collect the free parameters in $\mathfrak{B}$ to form

$$\underline{\beta}^T = [\beta_1, \ldots, \beta_n] \tag{60}$$

The necessary conditions for a local minimum of $\mathfrak{L}$ are

$$\frac{\partial \mathfrak{L}}{\partial P} = 0 \qquad \frac{\partial \mathfrak{L}}{\partial L} = 0 \qquad \frac{\partial \mathfrak{L}}{\partial \underline{\beta}} = 0 \tag{61}$$

which gives

$$\frac{\partial \mathfrak{L}}{\partial P} = \bar{\Phi}^T L \bar{\Phi} - L + M = 0 \tag{62}$$

Eq. (46) for $\partial \mathfrak{L}/\partial L$, and

$$\left(\frac{\partial \mathfrak{L}}{\partial \underline{\beta}}\right)_i = 2e_i^T\left[NP\Phi^T L\Pi + \Pi^T L \Pi \mathfrak{B} NPN^T\right]e_i = 0 \tag{63}$$

for $i = 1, \ldots, n$. In Eq. (63), e_i is the ith standard basis vector of $\mathfrak{R}^n$, so that evaluation of $\partial \mathfrak{L}/\partial \underline{\beta}$ consists of picking off the main diagonal entries of the quantity in brackets. We will also require the quantity

$$\mathfrak{IC} \equiv \frac{\partial^2 \mathfrak{L}}{\partial \underline{\beta} \partial \underline{\beta}^T} \tag{64}$$

where

$$\frac{\partial^2 \mathfrak{L}}{\partial \underline{\beta}_i \partial \underline{\beta}_j} = (\Pi^T L \Pi)_{ij}(NPN^T)_{ij} \tag{65}$$

A simple numerical algorithm for solving the necessary conditions is given as follows.

1) Choose any value for $\underline{\beta}$ which results in a stable discretization. Set $k = 0$.

2) Solve Eqs. (46), and (62) for L_k and P_k.

3) Calculate $\partial \mathfrak{L}/\partial \underline{\beta}_k$ from Eq. (63) and $\mathfrak{IC}_k$ from Eq. (64).

4) Set

$$\underline{\beta}_{k+1} = \underline{\beta}_k - \epsilon \mathfrak{IC}_k^{-1}\left(\frac{\partial \mathfrak{L}}{\partial \underline{\beta}_k}\right) \tag{66}$$

where $\epsilon \in (0, 1]$ is chosen to ensure that

$$J_{k+1} < J_k = \mathrm{tr}\{P_k M\} \tag{67}$$

5) Set $k = k + 1$ and go to step 2.

This algorithm is an analog of an efficient, proven approach for calculating optimal output feedback regulator gains, whose convergence is well documented.[10,11] For step 4 of the provided algorithm, we require that $\mathfrak{IC} > 0$, for invertibility and to ensure that $-\mathfrak{IC}^{-1}(\partial \mathfrak{L}/\partial \underline{\beta})$ is a descent direction for J. The following lemma establishes a sufficiency condition for this which does not impose significant restrictions for practical simulator designs.

Lemma: Assume that asymptotically stable $\bar{\Phi}$ has no zero eigenvalues. If $\{\bar{\Phi}, Z\}$ is controllable, and $\{M, \bar{\Phi}\}$ is observable, where

$$Z = \frac{(1-\alpha)}{\Delta t}\Theta + \alpha X_0 \qquad \alpha \in [0, 1] \tag{68}$$

then $\mathfrak{IC} > 0$.

Proof: See the Appendix.

Loosely speaking, this lemma states that, as long as we specify input and environmental noise which excites all of the plant, prefilter, and discretization modes, and choose the system outputs such that all system modes are observable from the error signal $e(t)$, then $\mathfrak{IC} > 0$.

IV. Application

In this section, optimized two-step [Eq. (48)] discretizations are designed for simulating the rigid-body blade dynamics of a helicopter with a fully articulated rotor. The plant model is generic, but patterned on the UH60 Blackhawk. Pertinent physical parameters are summarized in Table 1.

We consider the flapping and lead-lag degrees of freedom, illustrated in Fig. 1, for the case of no translational motion. Defining β to be the flap angle, ζ the lag angle, and θ the blade pitch angle, the dynamics are described by

$$\begin{aligned} &\ddot{\beta} + \Omega^2(1 + 3\bar{e}/2)\beta + 2\beta\dot{\zeta}\Omega \\ &\quad = \gamma\Omega^2/8\left[\theta + 4\lambda/3 - \dot{\beta}/\Omega + (2\theta + 4\lambda/3)\dot{\zeta}/\Omega\right] \\ &\quad - 2\beta\dot{\beta}\Omega + \ddot{\zeta} + 3\bar{e}\Omega^2\zeta/2 \end{aligned} \tag{69}$$

$$\begin{aligned} &= \gamma\Omega^2/8\left[-(\theta + 8\lambda/3)\dot{\beta}/\Omega - (2\xi/a - 4\lambda\theta/3)\dot{\zeta}/\Omega\right. \\ &\quad \left. - B_D\dot{\zeta}/I_B - \xi/a + 4\lambda\theta/3 + 2\lambda^2\right] \end{aligned} \tag{70}$$

where $\bar{e} = e/R$ is the normalized hinge offset. These expressions were adapted from Ref. 12, and differ only in that a viscous lag damper has been included in Eq. (70). The variable

Table 1 Rotor system parameters

Parameter	Symbol	Value
Weight, lb	W	16400.0
Main rotor radius, ft	R	26.83
Blade chord, ft	c	1.73
Rotor angular rate, rad/s	Ω	27.00
Blade moment of inertia, slug × ft^2	I_B	1507.4
Viscous lag damper coefficient, slug × ft^2/s	B_D	1500.0
Number of blades	b	4
Blade lift curve slope, 1/rad	a	5.73
Lock number, $\rho acR^4/I_B$	γ	8.194
Solidity, $bc/\pi R$	σ	0.0821
Blade drag coefficient	ξ	0.00936
Flap hinge offset, ft	e	1.25
Sea level air density, slug/ft^3	ρ	0.00238

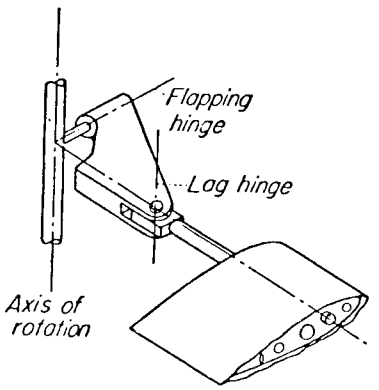

Fig. 1 Flapping and lag degrees of freedom.

λ represents the effect of induced velocity and is related to the thrust coefficient C_T by

$$\lambda = -(C_T/2)^{1/2}$$
$$C_T = T/\rho\pi R^4\Omega^2 = a\sigma(\theta/3 + \lambda/2)/2 \tag{71}$$

The linearized plant model for the optimization was calculated for hovering flight about equilibrium values of β and ζ satisfying

$$\beta_0 = \frac{\gamma}{8(1+3\bar{e}/2)}\left[\theta_0 + \frac{4\lambda}{3}\right] \tag{72}$$

$$\zeta_0 = \gamma\left[-\zeta/a + 4\lambda_0\theta_0/3 + 2\lambda_0^2\right]/12\bar{e} \tag{73}$$

with λ_0, θ_0, and C_T^0 computed from Eq. (71) with T set equal to the vehicle weight.

The simulation of Eqs. (69) and (70) is assumed to have θ as the input, and β and ζ as separate outputs. The input is passed through a second-order Butterworth prefilter, whose cutoff frequency is set equal to the system sampling frequency. The outputs are converted to analog signals by zero-order holds

$$\hat{y}(\tau) - C\hat{x}_k \qquad \tau \in [k\Delta t,\ (k+1)\Delta t)$$

The homogeneous response of β and ζ to a step in θ is simulated. The input dynamics $\{A_u, B_u, C_u\}$, then, are modeled as the homogeneous response of a pure integrator to an initial condition uniformly distributed on the unit sphere. Since the design theory requires asymptotic stability, the integrator is approximated by a first-order lag with a time constant of 0.01. For simplicity, it is assumed that environmental noise effects are negligible.

The classical discretization formula most similar to the optimized two-step formulas treated in this paper is the second-order Adams-Bashforth (AB2)

$$\hat{x}_{k+1} = \hat{x}_k + \Delta t\left[1.5\hat{x}'_k - 0.5\hat{x}'_{k-1}\right]$$

Figures 2–5 display the simulation response to a 3-deg step in θ applied at 0.05 s, for AB2 and optimized discretizations. The solid line in each of the figures is the plant trajectory obtained using an accurate integration routine, and the broken line is the simulation response, reconstructed with zero-order hold. Figure 2 shows the response of an AB2 discretization at 35-Hz sampling. At this sampling frequency, the flapping response of the AB2 discretization shows spurious underdamping, warning that the sampling frequency cannot be reduced much further. This is supported by Fig. 3, which displays the response for the same configuration with 30-Hz sampling, plainly showing serious instability.

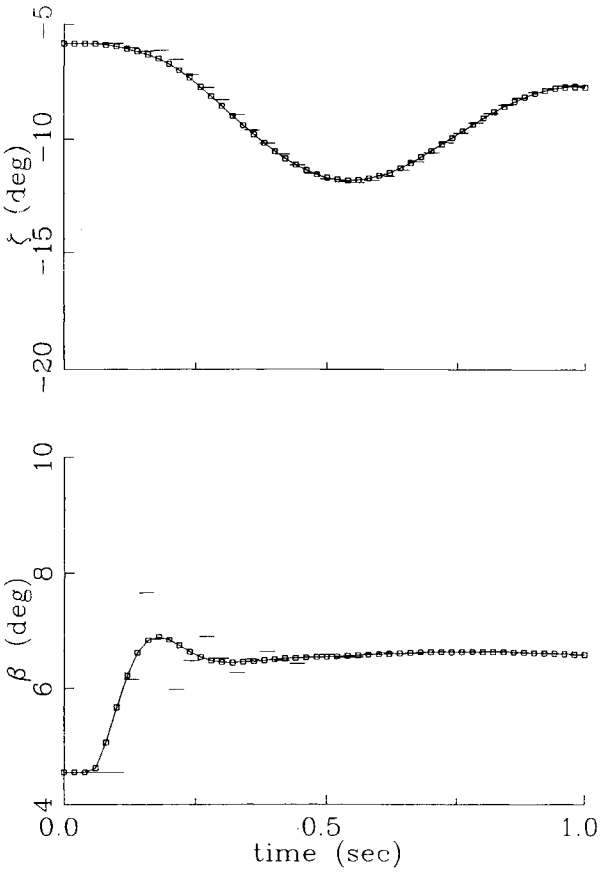

Fig. 2 AB2 discretization and 35 Hz sampling frequency.

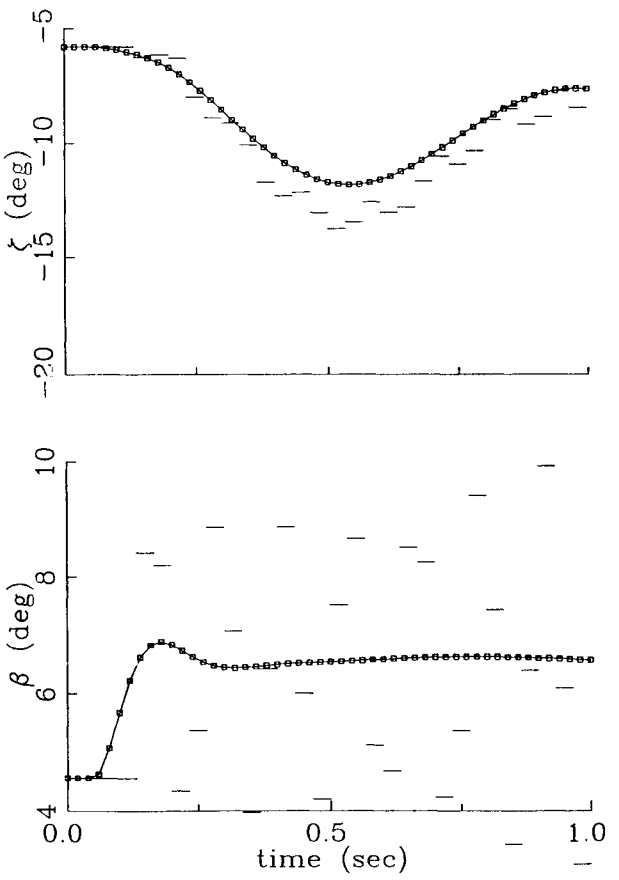

Fig. 3 AB2 discretization and 30 Hz sampling frequency.

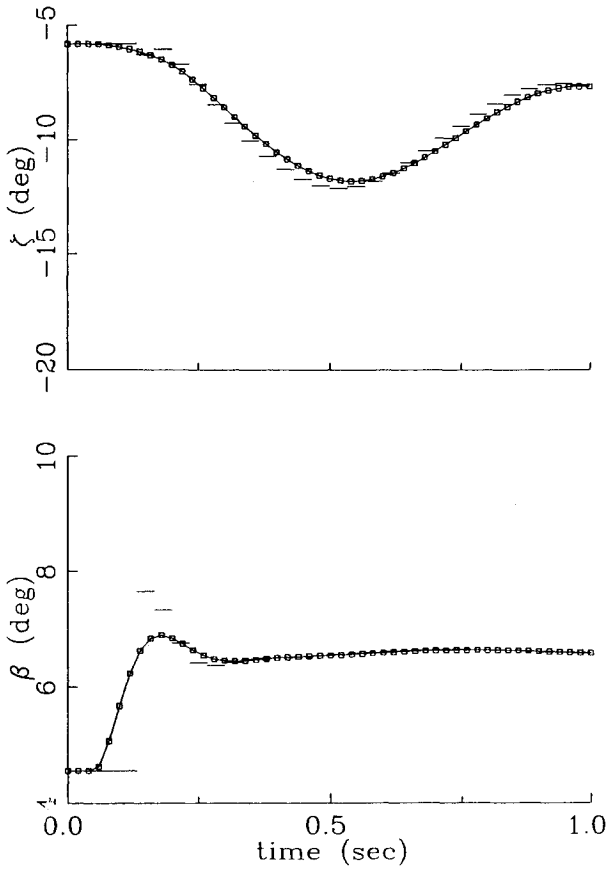

Fig. 4 Optimal discretization for 30 Hz sampling frequency.

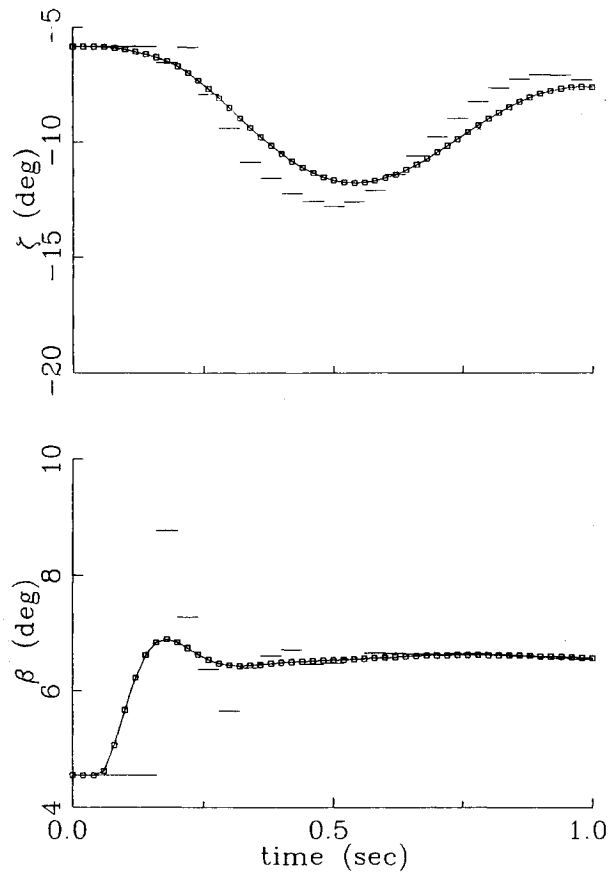

Fig. 5 Optimal discretization for 25 Hz sampling frequency.

Optimized discretizations of the form Eqs. (48–50) were calculated for sampling frequencies of 30 Hz and 25 Hz. For 30 Hz, the discretization coefficients were

$$\underline{\beta} = [1.78325, 1.00791, 1.65778, 1.41291]$$

and, for 25 Hz,

$$\underline{\beta} = [1.75576, 0.91654, 1.66885, 1.42628]$$

Figures 4 and 5 show simulation time histories for the 30-Hz and 25-Hz optimized discretizations. In Fig. 4, aside from a brief overshoot in flapping angle, the response appears very well behaved and tracks the accurate trajectory quite well. This is significant since the slower sampling required by the optimized discretization makes proportionately smaller demands on computing power for real-time implementation. The response for the 25-Hz discretization in Fig. 5 shows some noticeable underdamping; however, it is quite comparable to the AB2 response at 35 Hz.

Conclusions

This paper has treated quantification of fidelity in digital real-time simulations, and the derivation of efficient discrete-time representations of plant dynamics for use in them. A performance criterion was derived which expresses the simulation fidelity in terms of the time-domain discrepancy between the actual and simulated plant outputs, given identical probabilistically distributed input signals and/or initial conditions, under an assumption that the plant dynamics are linearizable and asymptotically stable. The performance criterion was used as a cost function in a simple procedure for optimizing free parameters in discretizations based on a generalized form of one- and two-step open linear numerical integration formulas. Optimal two-step discretizations were calculated for simulating the nonlinear rigid-body dynamics of a helicopter rotor blade system. The technique permitted a roughly 29% decrease in sampling frequency as compared to a discretization based on a classical second-order Adams Bashforth integration formula.

Appendix: Proof of Lemma

Let ρ be the dimension of $\bar{\Phi}$ and Z. Since $\{\bar{\Phi}, Z\}$ is controllable, the matrix

$$\mathfrak{M} = \left[\bar{\Phi}^{\rho-1}z : \bar{\Phi}^{\rho-2}z : \cdots : z\right] \tag{A1}$$

has full rank. The nonsingularity of $\bar{\Phi}$, then, implies that

$$\mathfrak{M}' = \left[\mathfrak{M}'_{\rho-1} : \mathfrak{M}'_{\rho-2} : \cdots : \mathfrak{M}'_0\right] \tag{A2}$$

$$\mathfrak{M}'_j = \bar{\Phi}^j z \bar{\Phi}^{jT} \tag{A3}$$

has full rank. Represent each $\mathfrak{M}'_j$ as

$$\mathfrak{M}'_j = \sum_{i=1}^{p} \lambda_{ij} v_{ij} v_{ij}^T \tag{A4}$$

where $\lambda_{ij} > 0$ and p is the rank of $\mathfrak{M}'_j$, and define

$$\tilde{P} = \sum_{j=1}^{\rho} \mathfrak{M}'_j \tag{A5}$$

Because there are ρ linearly independent v_{ij}, it is obvious that $\tilde{P} > 0$. This implies that $P > 0$, where, from Eq. (46),

$$P = \lim_{N\to\infty} \sum_{k=0}^{N} \bar{\Phi}^k z \bar{\Phi}^{kT} \tag{A6}$$

by substitution. Similar reasoning yields $L > 0$.

From Eqs. (53) and (56), Π has full rank, so that $\Pi^T L \Pi > 0$.

Similarly, in Eqs. (54) and (57), N has full rank, since A is asymptotically stable. Therefore, $NPN^T>0$ and $\tilde{\mathcal{K}}>0$, where

$$\tilde{\mathcal{K}} \equiv (\Pi^T L \Pi) \otimes (NPN^T) \tag{A7}$$

Define $\tilde{\mathcal{K}}_k$ by

$$\tilde{\mathcal{K}}_k = E_k \tilde{\mathcal{K}}_{k-1} E_k^T \qquad k = 2, \ldots, n$$
$$\tilde{\mathcal{K}}_1 = \tilde{\mathcal{K}} \tag{A8}$$

where E_k is the elementary matrix which interchanges rows k and $(k-1)n+k$. The upper left $n \times n$ partition of $\tilde{\mathcal{K}}_n$ is $\tilde{\mathcal{K}}$. Since $\tilde{\mathcal{K}}_n > 0$, all of its leading principal minors are positive, so that all of the leading principal minors of $\mathcal{K}$ are positive. Therefore, $\mathcal{K}>0$.

References

[1]Sage, A., and Smith, S., "Real-Time Digital Simulation for Systems Control," *Proceedings of the IEEE,* Vol. 54, No. 12, Dec. 1966, pp. 1802–1812.

[2]Fowler, M., "A New Numerical Method for Simulation," *Simulation,* Vol. 6, Feb. 1966, pp. 90–92.

[3]Smith, J., *Mathematical Modeling and Digital Simulation for Engineers and Scientists,* Wiley, New York, 1977.

[4]Nigro, B., "An Investigation of Optimally Stable Numerical Integration Methods with Application to Real-Time Simulation," *Simulation,* Vol. 19, Nov. 1969, pp. 253–264.

[5]Barker, L., Bowles, R., and Williams, L., "Development and Application of a Local Linearization Algorithm for Integration of Quaternion Rate Equations in Real-Time Flight Simulation Problems," NASA TN-D-7347, Dec. 1973.

[6]Gear, C. W., "Simulation: Conflicts Between Real-Time and Software," *Mathematical Software III,* edited by J. R. Rice, Academic, New York, 1977.

[7]Rolston, D., "Sinusoidal Integration for Simulation of Second-Order Systems," *Proceedings of the AIAA Flight Simulation Technical Conference* (Niagara Falls, NY), AIAA, New York, June 1983.

[8]Moerder, D., Halyo, N., and Broussard, J., "Measures of End-to-End Fidelity for Digital Real-Time Simulation," Information and Control System, Inc., Final Rept. 685102, Hampton, VA, Sept. 1985.

[9]Gear, C. W., *Numerical Initial Value Problems in Ordinary Differential Equations,* Prentice-Hall, Englewood Cliffs, NJ, 1971, pp. 169–187.

[10]Halyo, N., and Broussard, J., "A Convergent Algorithm for the Stochastic Infinite-Time Optimal Output Feedback Problem," *Proceedings of the Joint Automatic Control Conference,* Paper No. WA-1E, Charlottesville, VA, June 1981.

[11]Moerder, D., and Calise, A., "Convergence of a Numerical Algorithm for Calculating Optimal Output Feedback Gains," *IEEE Transactions on Automatic Control,* Vol. AC-30, No. 9, 1985, pp. 900–903.

[12]Dowell, E., Curtiss, H., Scanlan, R., and Sisto, F., *A Modern Course in Aeroelasticity,* Sijthoff & Noordhoff, Rockville, MD, 1980, pp. 327–382.